Advanced characterization of airbag fabrics for *MAT_FABRIC including permeability

Daniel Muñoz[1], Alberto Regidor[1], Javier Ferrer[1]

[1]Newgentechs

ABSTRACT

The airbag fabric is a highly complex material and has a great influence on the behavior of the restraint system in crashworthiness events. LS-DYNA offers multiple possibilities to simulate it, including dependencies with triaxiality, strain rate or permeability, among others.

To take advantage of these capabilities, a highly specialized experimental characterization program, including different types of mechanical loading and specific permeability tests is required.

Dynamic permeability tests used so far for the characterization of airbag fabrics have been limited to low pressures and room temperature. At Newgentechs, an experimental system has been developed to reproduce the high pressures encountered in the airbag at the earliest stages of the opening and at different temperatures, providing new information on the behavior of these materials.

This presentation describes state-of-the-art experimental and analytical techniques for characterizing airbag fabrics for simulation, including this new system for determining permeability.

1 Introduction, target and methods

Fabrics play a crucial role in critical components of automotive restraint systems such as airbags and seat belts, where their mechanical performance directly affects occupant safety. These fabrics are typically composed of bundles of polymeric filaments woven in two orthogonal directions (warp and weft), sometimes including coating layers to improve thermal resistance, control air permeability, or reduce porosity.

Under typical impact scenarios, airbag fabrics experience a wide range of loading conditions. The internal pressure rises sharply to very high values at the moment of ignition, falls rapidly as the bag leaves its housing, and then stabilizes at intermediate and more uniform levels once the airbag has fully deployed. Strain rates range from extremely high during the initial unfolding to quasi-static after deployment. The types of mechanical loads also vary, from localized uniaxial stresses in straps and other constrained zones to biaxial stresses generated by the volumetric inflation pressure. In addition, fabrics are exposed to temperature effects related to both environmental temperature and to the hot gases released by the inflator. These diverse and transient conditions demand a detailed material characterization to ensure that the mechanical response of fabrics can be accurately reproduced in numerical models.

The deployment of an airbag is a highly dynamic process that can be divided into four main phases (Fig. 1). In the first phase, from ignition to cover opening, the folded fabric is exposed to heterogeneous and locally high pressures with very high strain rates near the inflator. During the deployment or slash phase, the bag unfolds rapidly, still under high strain rates but generally low internal pressures. In the filling phase, the airbag reaches its full volume, experiencing lower strain rates while pressure rises from low to intermediate levels. Finally, in the filled and restraint phase, the airbag stabilizes with quasi-static or low strain rates and homogeneous intermediate pressures, ready to receive the occupant. The evolution of internal pressure, volume, kinetic energy, and fabric strain illustrates the strong variability of loading conditions across these phases.

To lead with these phenomena, LS-DYNA offers dedicated constitutive models for airbag fabrics [1]. The *MAT_034 / *MAT_FABRIC law is the most widely used, allowing the definition of uniaxial and biaxial tensile behavior in warp and weft directions, as well as shear response, primarily through experimental curves. Strain rate effects can be introduced by tables, while temperature effects require separate cards. This formulation remains the industrial reference. The more recent *MAT_034M / *MAT_FABRIC_MAP [1][2] provides greater flexibility, combining different load cases and simplifying

the definition of hysteresis and strain rate through parameters or scaling factor curves. Moreover, temperature effects can be directly introduced by tables, making it a more advanced and versatile option. However, its use is nowadays much less widespread than that of *MAT_FABRIC, at least to the author's knowledge.

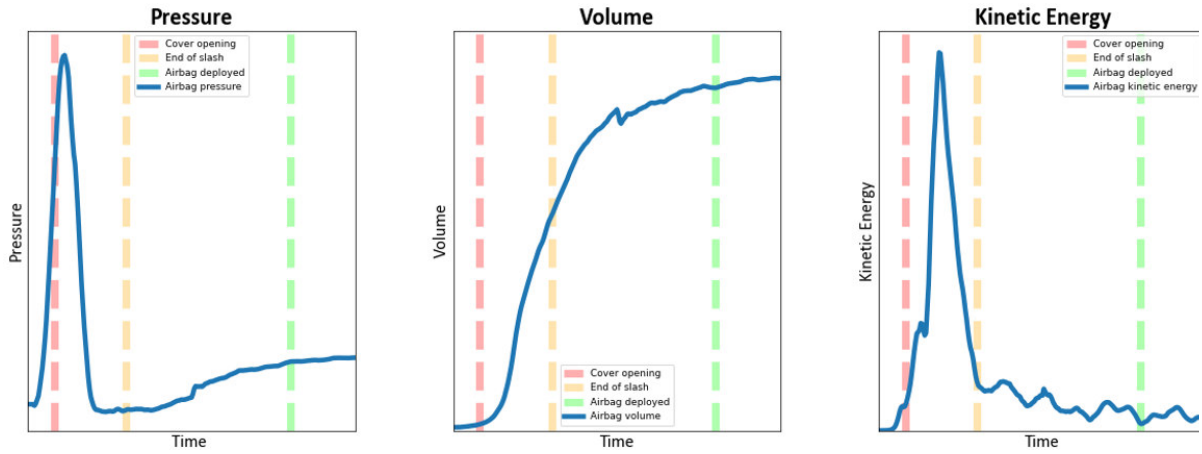

Fig.1: Evolution of airbag variables defining the different phases of an airbag deployment

To further investigate and illustrate fabric performance under such conditions, a set of LS-DYNA models of a fictitious driver airbag have been specifically developed for this study (Fig. 2). The aim was to use a base model representative enough of a real airbag, while avoiding any association with commercial products or brands. The models feature a generic geometry with unstructured folding, enclosed within a basic environment. A combination of data from different sources including materials, inflator characteristics, and boundary conditions, has been used. Two alternative airbag formulations were considered: (i) the Corpuscular Particle Method (CPM), defined through *AIRBAG_PARTICLE with 200,000 particles and transitioning to uniform pressure after 25 ms, and (ii) the Uniform Pressure (UP) method, using a similar definition, but changing to uniform pressure at the start of the simulation. Both were evaluated under different load cases, including deployment, restraint performance and aggressiveness in out-of-position (OOP) scenarios.

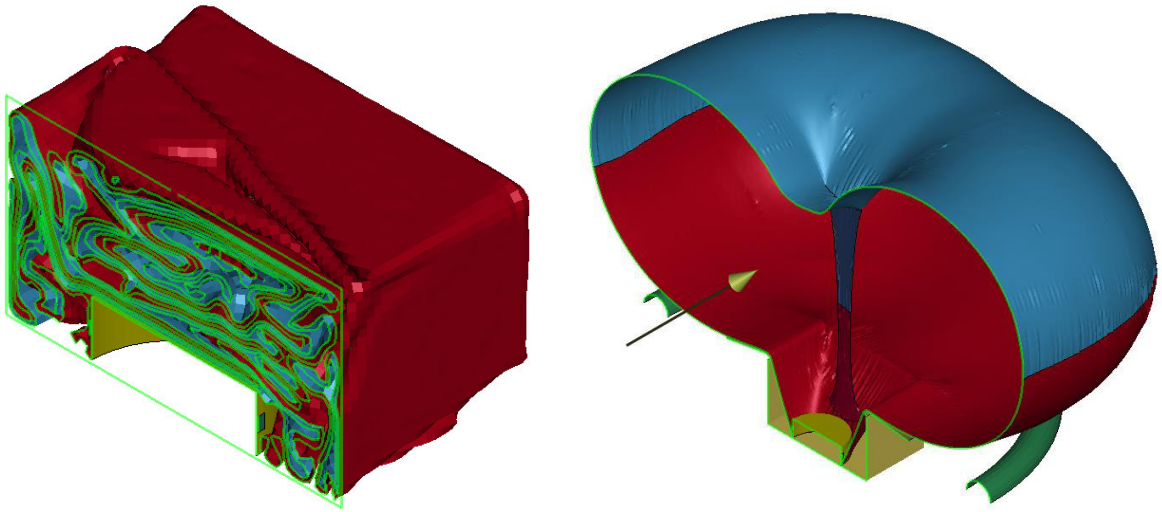

Fig.2: Section views of the folded and unfolded sample airbag models generated for the study

The aim of this work is to present advanced experimental and numerical methods for characterizing airbag fabrics and to evaluate the impact of different modeling approaches in realistic applications. Although the focus is on airbags, many of these methodologies are also applicable to seat belts.

Particular emphasis will be placed on the *MAT_034 material law, due to its much more extended use, although the most of these methods can also be used for *MAT_034M.

2 Uniaxial vs. Biaxial Loads in Fabric Materials

The mechanical response of woven fabrics is strongly influenced by the interaction between fibers in the two principal directions, warp and weft. LS-DYNA material models *MAT_FABRIC and *MAT_FABRIC_MAP take into account this interaction, which has a major effect on material behavior. When both directions are simultaneously loaded, the fibers mutually constrain each other, resulting in a higher stiffness and an earlier failure compared to uniaxial loading conditions.

A simplification of this effect can be conceptually explained by considering the straightening of fibers (see Fig. 3). Under uniaxial tension, the unloaded transverse fibers allow the loaded direction to elongate more freely. In contrast, under biaxial tension, both directions are simultaneously stretched, restricting fiber reorientation and increasing the resistance to deformation. As a result, the material exhibits higher effective stiffness and lower effective strain at failure under biaxial loading.

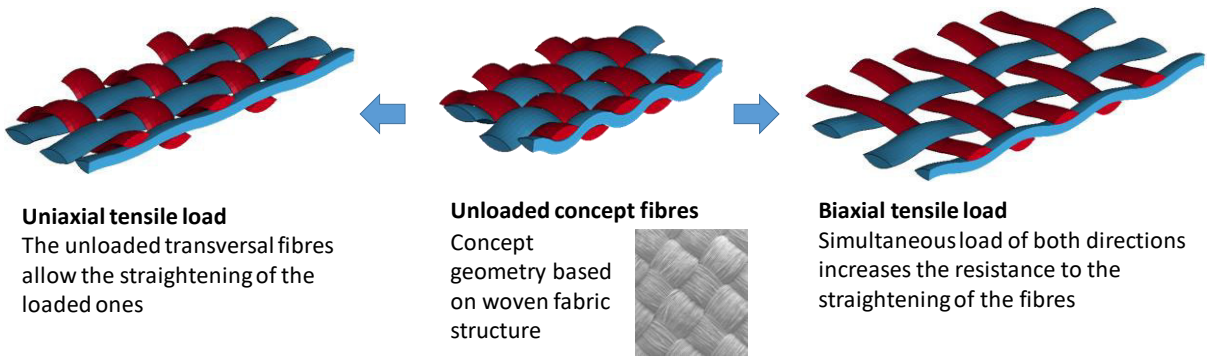

Fig.3: Conceptual explanation of differences between uniaxial and biaxial loads in a fabric.

A sample of the effective influence measured on a real fabric can be seen in Fig 4.

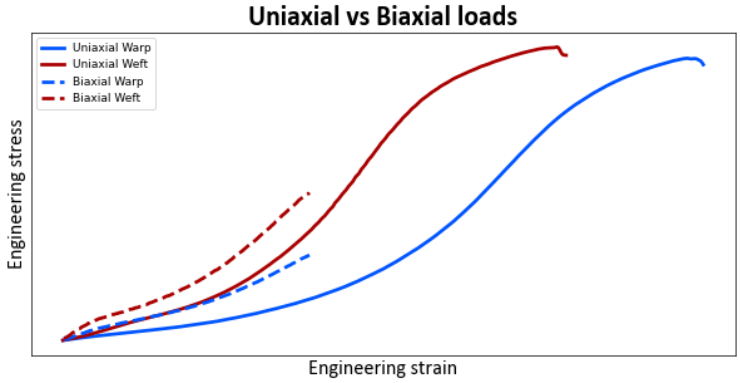

Fig.4: Sample of uniaxial vs biaxial behavior in a real material (quasi-static tests up to failure).

In practice, both uniaxial and biaxial stresses are present during the deployment of an airbag. Uniaxial loads are typically associated with localized features such as straps, local constraints, or heterogeneous stress distributions during the early unfolding phase. Biaxial loads, on the other hand, become dominant in rounded regions of the airbag, where uniform gas pressure and lack of other constraints produce quasi-spherical geometries after deployment. Additionally, the load state evolves dynamically throughout the deployment process. During ignition and unfolding, the stress distribution is heterogeneous and uniaxial effects are more significant. As the airbag inflates and reaches its final shape, biaxial loads prevail, defining the mechanical state of the fabric during the restraint phase. An approximated view of these effects can be done in the simulation models by means of the triaxiality (See Fig. 5).

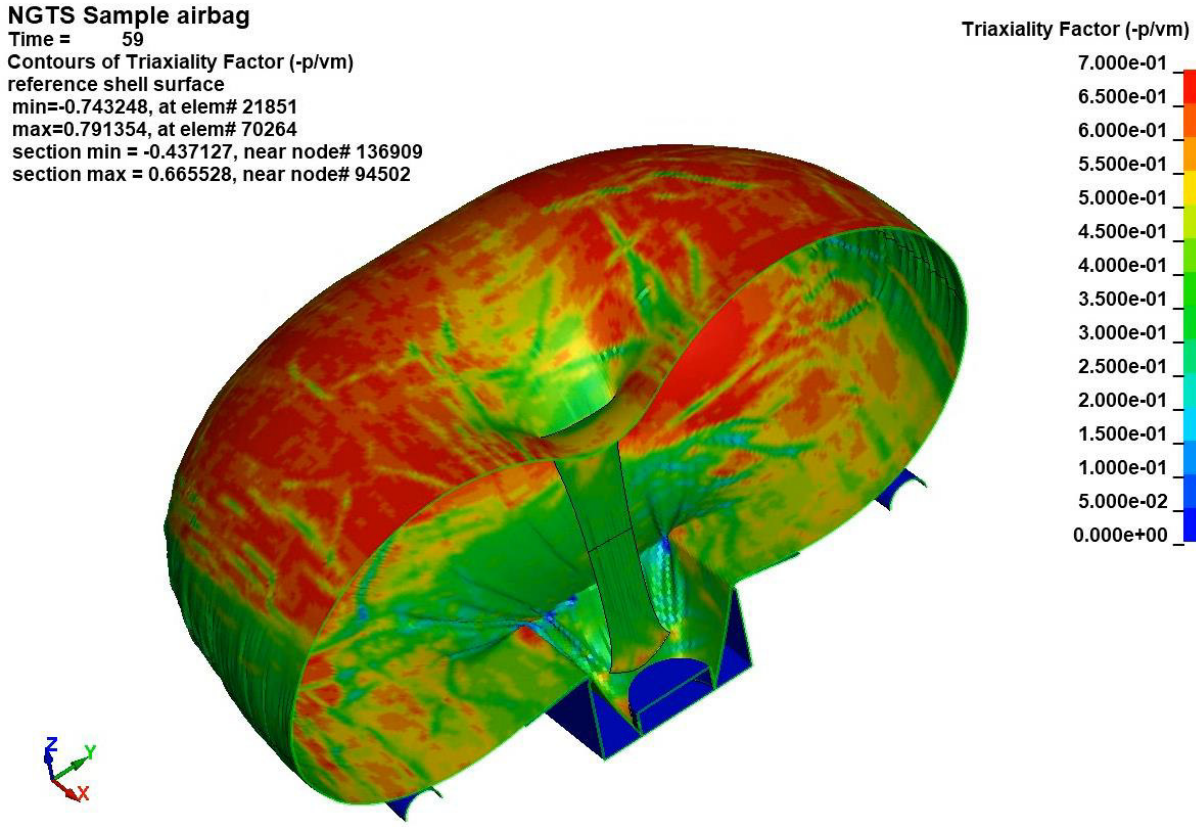

Fig.5: Deployed sample airbag (section view) with contours of triaxiality factor. Green color (close to 0.33) is related to a higher influence of uniaxial loads and red color (close to 0.66) implies a higher influence of biaxial loads.

3 Strain rate dependence

Airbag fabrics experience significant strain rate variations throughout the deployment process. The opening and slash phases are characterized by very high strain rates, particularly in regions close to the inflator and straps, whereas in the later phases, the overall strain rates decrease and the fabric response becomes generally much slower. Numerical simulations allow these variations to be quantified, providing detailed information on the evolution of strain and strain rate at different locations of the airbag. Fig. 6 shows an estimation of the strain rate at different locations of the airbag. This estimation has been done by means of the derivative of the history variable 28 (Effective Strain (Von Mises)) available in the *MAT_034.

Airbag fabrics are typically strain rate dependent materials. Fig. 7 displays some characterization tests results performed at different speeds, as a sample of this dependence. Consequently, as a general rule, it is desirable to have an adequate representation of these effects in material models in order to increase their predictive capability.

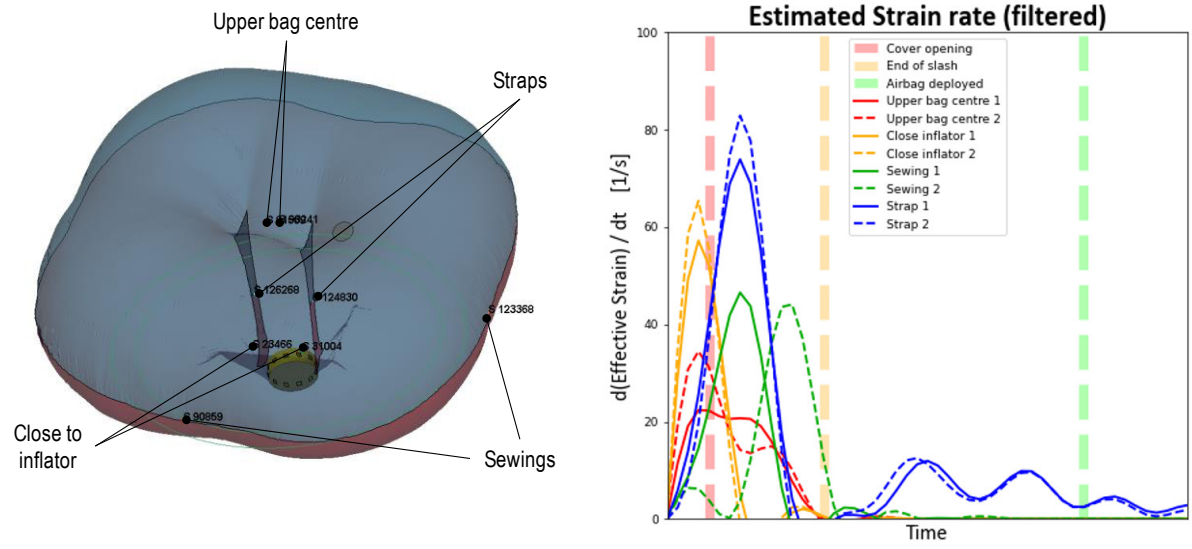

Fig.6: Estimation of strain rates at different locations during the airbag deployment (from sample airbag simulation using CPM)

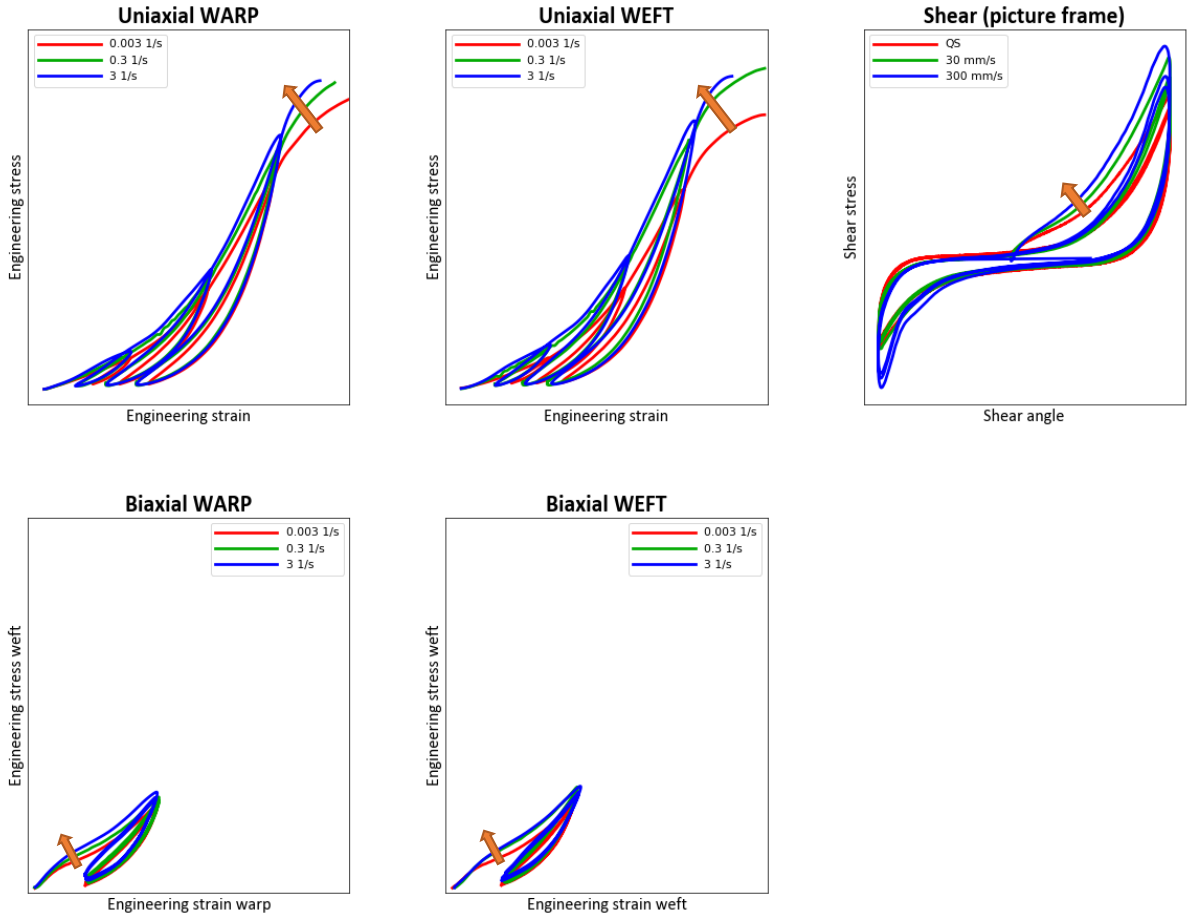

Fig.7: Sample strain rate dependence for different load states. Cyclic tests not conducted up to failure are represented. For comparison purposes, all the tensile tests (uniaxial and biaxial) are plotted with the same scale.

In order to take strain rate effects into account in the material characterization, stress–strain–strain rate surfaces (3D surfaces) are adjusted from experimental data (see Fig. 8). This approach enables the definition of stress–strain curves at constant strain rates while incorporating the variations observed during testing. This methodology is also used with other strain rate dependent LS-DYNA material models (e.g., *MAT_024, *MAT_SAMP-1) [3][4] and provides with many advantages, like the inclusion of strain rate dependence directly in the fitted surfaces, the possibility of interpolation and extrapolation beyond the experimentally tested rates, the capability of getting a number of effective curves higher than those directly measured and the possibility to operate directly with surfaces to extrapolate and get new surfaces for some applications.

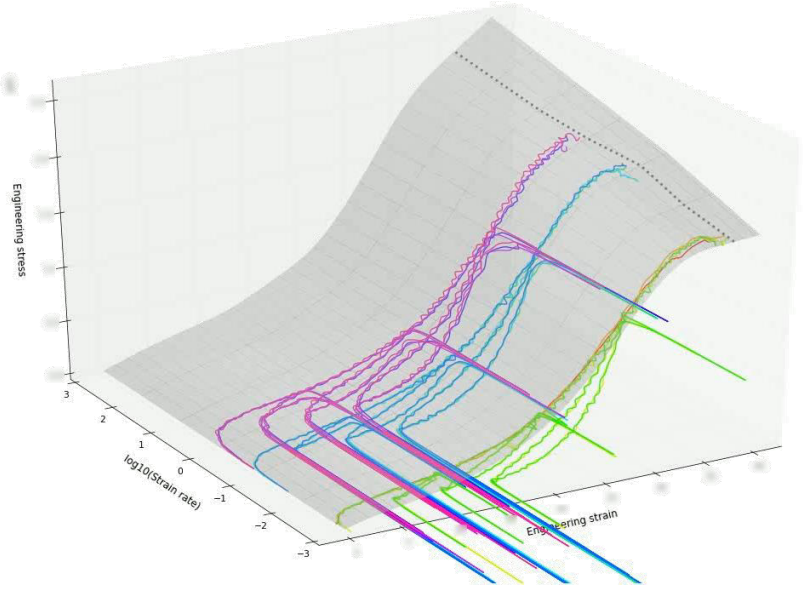

Fig.8: Sample 3D surface adjusted from uniaxial tensile tests of an airbag fabric.

In the case of fabrics, the method to adjust the surfaces was adapted to remove unload and reload phases from the experimental cycles, focusing solely on the monotonic response. In the case of *MAT_FABRIC, this technique is used to define up to four independent surfaces to create different tables: uniaxial warp (LCA), uniaxial weft (LCB), biaxial warp (LCAA), and biaxial weft (LCBB). These surfaces serve as a seed for the later iterative adjustment of the model based on the simulation results.

This strategy allows a robust and flexible representation of the material behavior, ensuring that the strain rate dependence of fabrics is adequately captured in LS-DYNA simulations of airbag deployment.

4 Temperature dependence

In addition to strain rate effects, airbag fabrics are also sensitive to temperature. During deployment, the material is subjected to two types of thermal influences:

- Climatic conditions, associated with the initial environmental temperature.
- Transient heating, produced by the hot gases released from the inflator, which produce complex effects including a progressive heating of the fabric material.

To properly account for these influences, mechanical tests are carried out at controlled temperatures by attaching climatic chambers to the testing machines. This approach enables the experimental determination of stress–strain curves under representative environmental conditions. Results typically show a clear temperature dependence: higher stiffness and strength at low temperatures, and reduced performance as the temperature increases. A sample of this dependence can be seen at Fig. 9.

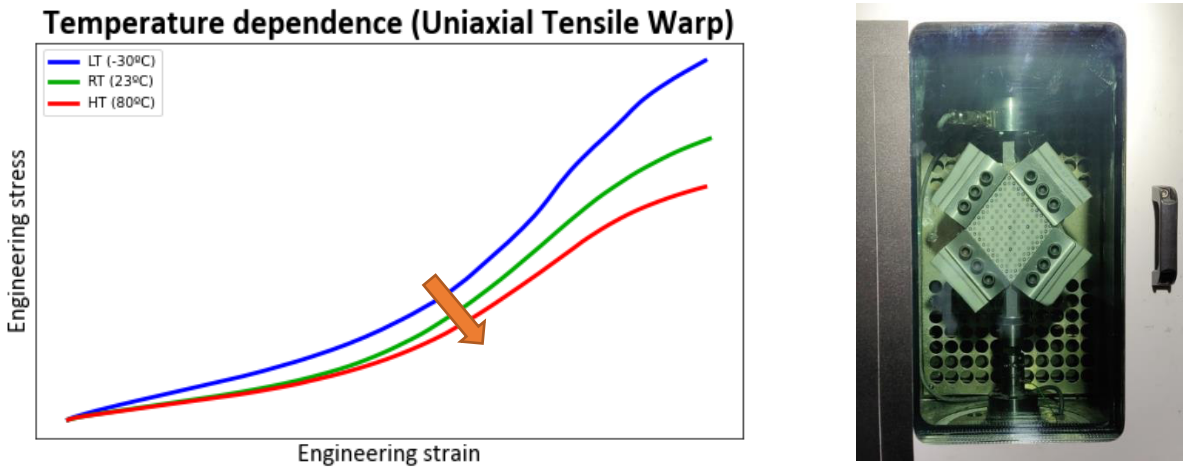

Fig.9: Temperature dependence found on a sample case and characterization test performed within a climate chamber coupled to the testing machine.

In LS-DYNA, *MAT_FABRIC material model does not directly include temperature dependence. Instead, separate sets of material cards must be generated for each tested temperature. On the other hand, *MAT_FABRIC_MAP introduces the temperature dependence in its formulation.

5 Typical mechanical tests on airbag fabrics

The characterization of airbag fabrics requires a combination of experimental tests that reproduce the different loading modes acting on the material during deployment. Three main types of tests are the most typically used (as displayed at Fig. 10):

- **Uniaxial tensile tests** (warp and weft directions): Fabric strips aligned with the warp or weft directions are tested under tension. Both monotonic loading up to failure and cyclic loading–unloading tests are conducted. Tests are carried out at different strain rates and under controlled temperatures, in order to capture the combined effects of rate dependence and thermal sensitivity. These tests are directly related to the LCA, LCB, LCUA and LCUB parameters in the *MAT_FABRIC.

- **Biaxial tensile tests**: Cross-shaped specimens are subjected to simultaneous loading in both warp and weft directions. Different strain rates, temperature conditions, and warp-to-weft load ratios can be applied, allowing a comprehensive exploration of the biaxial response. In *MAT_FABRIC (FORM -14) these tests can add complementary information to the uniaxial tests by means of the parameters LCAA and LCBB, or even substitute them if they are used to adjust the tables LCA and LCB directly, if the influence between uniaxial and biaxial loads is decided to be neglected. Also, the biaxial information can be selected instead of the uniaxial one to adjust the unload curves LCUA and LCUB. For the case of *MAT_FABRIC_MAP, different load ratios can be applied to the warp and weft directions.

- **Shear tests (picture frame method):** Cross-shaped specimens are loaded in shear using an articulated picture-frame fixture. The tests include cyclic loading–unloading sequences and can be performed at different strain rates and temperatures. An alternative but less direct method to produce a shear loading of the material is the uniaxial tensile tests aligned at 45º with regards to the warp and weft directions. In *MAT_FABRIC these tests are aimed to adjust the curves LCAB and LCUAB.

The combination of these tests ensures that the material characterization covers the wide range of loading states experienced by airbag fabrics, from uniaxial strap stresses to biaxial inflation pressures and in-plane shear during folding and deployment.

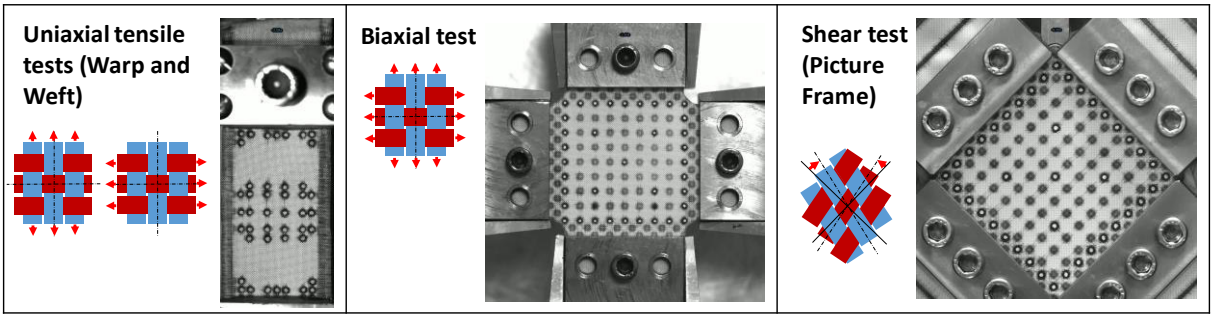

Fig.10: Most typical mechanical tests performed on airbag fabrics.

6 Dynamic permeability of Airbag Fabrics

Permeability is a key property of airbag fabrics, as it controls the gas leakage through the textile during and after deployment. In LS-DYNA, permeability is modeled as pressure-dependent, typically using the FAC curve in *MAT_FABRIC. While the typical internal pressures of a fully deployed airbag are usually below 1 bar, local pressures during the early stages of deployment —particularly during cover opening— can be significantly higher, with estimates reaching up to 6 bar and above.

Conventional dynamic permeability tests are generally limited to pressures with maximum ranges of around 1 bar, which may underestimate the actual behavior of fabrics under deployment conditions. To address this limitation, a dedicated high-pressure test system was developed at Newgentechs, specifically designed to measure permeability up to 6 bar and more [5]. This capability makes it possible to characterize the airbag fabric response under realistic operating pressures including the opening of the cover, beyond the range of standard commercial systems.

The new system is based on a pressure vessel (Volume 1) and a test chamber (Volume 2) communicated by a valve, as described in ASTM D6476 [6], but adapted to withstand and control pressures exceeding 6 bar (see Fig. 11). Tests are performed with dry air, and the specimens can be conditioned at different temperatures outside the test chamber and driven into testing position in less than one second, ensuring that the thermal state is preserved at the start of the experiment.

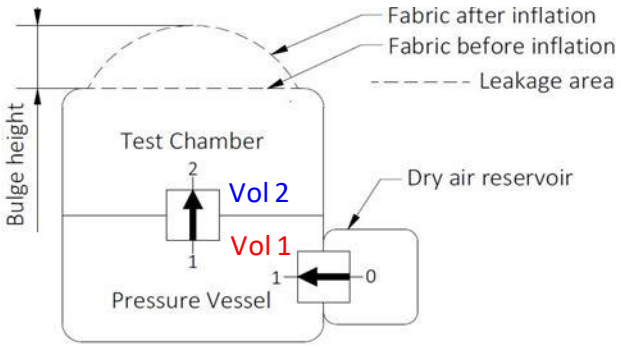

Fig.11: Basic scheme of the dynamic permeability test system.

Permeability is calculated from the pressures measured in both volumes, the bulge height, and the initial pressures and temperatures. At the beginning of the test, the Pressure Vessel is pressurized to the target level, while the Test Chamber remains at atmospheric pressure. When the valve is opened, the Test Chamber is rapidly filled, producing transient effects with non-uniform pressure fields that cannot be fully captured by the sensors. Once pressure equalizes in both chambers, the only gas exchange with the outside occurs through leakage across the tested fabric. At this point, the actual permeability calculation begins by monitoring the discharge from the system into the atmosphere (see Fig. 12). This setup enables the analysis of both pressure–time histories to estimate the evolution of permeability with pressure, providing direct input for the FAC curve in *MAT_FABRIC.

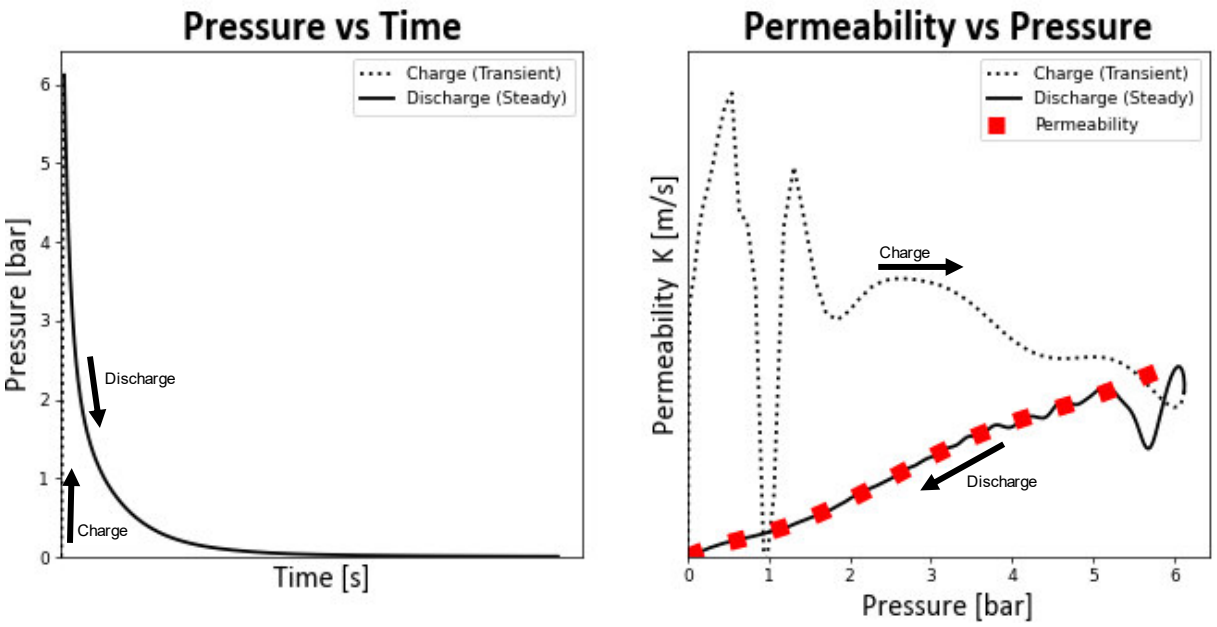

Fig.12: Basic scheme of the dynamic permeability test system.

7 LS-DYNA models for the material card adjustment

The experimental results obtained from the different tests are reproduced numerically in LS-DYNA in order to calibrate the material models. Calibration is performed through an iterative process, starting from initial “seed” curves and parameters that are progressively adjusted until good agreement with the experimental data is achieved. All test types are simulated and serve both for calibration and for validation of the numerical models.

Uniaxial and Biaxial Tests

In *MAT_FABRIC, the load response from uniaxial tensile tests in the warp and weft directions is defined using the rate-dependent tables LCA and LCB. When using FORM-14, the corresponding biaxial test results can also be introduced through the LCAA and LCBB tables. The unloading behavior is described by rate-independent curves (LCUA and LCUB), which are applied to both uniaxial and biaxial loading. Finally, reload effects and the energy dissipated in hysteresis cycles are governed by the parameter H.

Fig. 13 shows images of models reproducing the tensile tests (both uniaxial and biaxial) and typical results of an adjustment and validation process. The reproduction of the monotonic load of the material is typically well reproduced for all the load cases and strain rates, while, being the unload behavior limited to only one curve for each direction, a balance must be found for the reproduction hysteresis cycles. In the figure, the reproduction of the biaxial unloads at an intermediate speed has been prioritized over the uniaxial ones, but this criterion could change depending on the application.

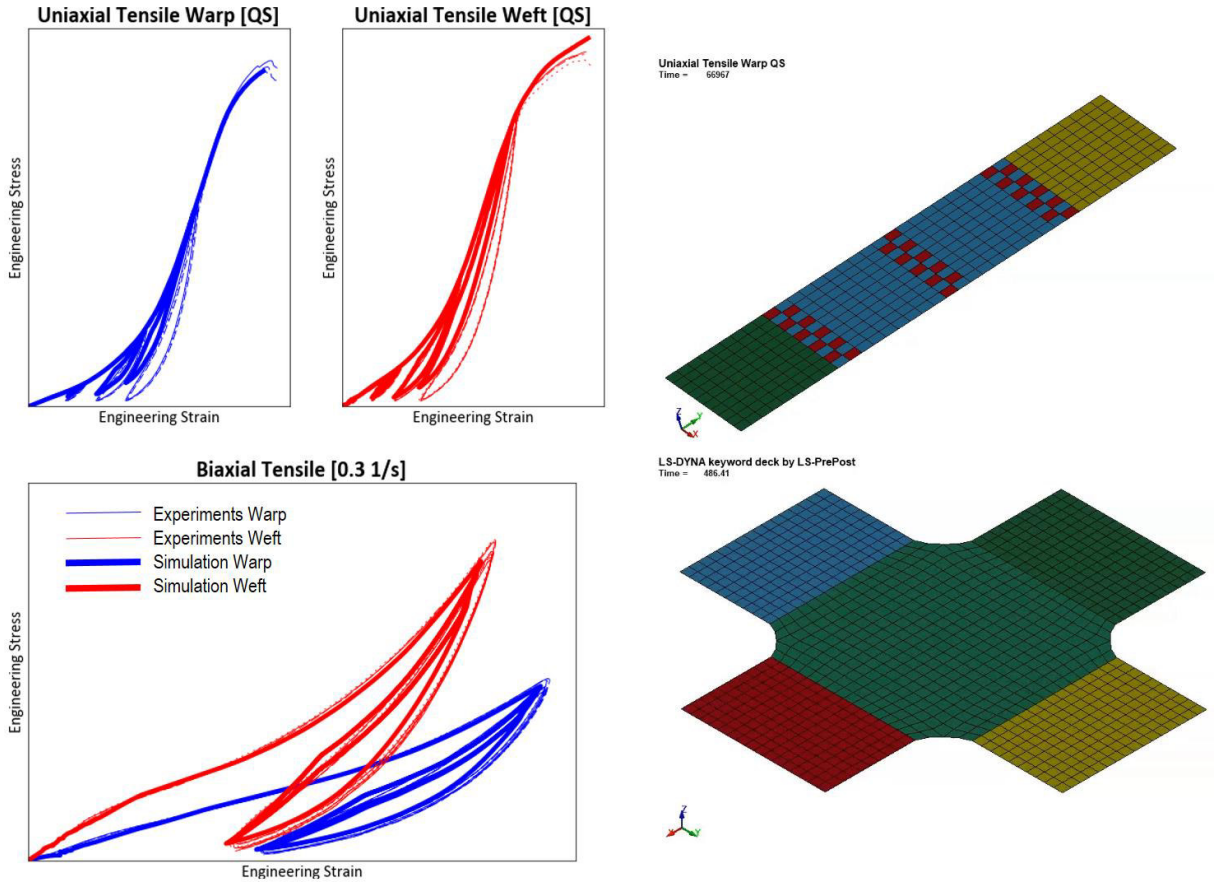

Fig.13: LS-DYNA models and typical validation results for uniaxial and biaxial tensile tests.

Shear Tests (Picture Frame)

Shear behavior is modeled using picture-frame test simulations (see Fig. 14). In this case, only strain-rate independent curves are available: LCAB for the initial loading phases and LCUAB for the combined unload–reload response. Since unloading and reloading are governed by the same curve, hysteresis cycles are not reproduced after the first unload. This requires the user to adopt a criterion to balance the reproduction of the different experimental effects. In the example shown in Fig. 14, priority was given to accurately reproducing the first load–unload cycle, although this results in a less accurate description of subsequent cycles. Depending on the application, alternative criteria may be selected to better capture the behavior of interest.

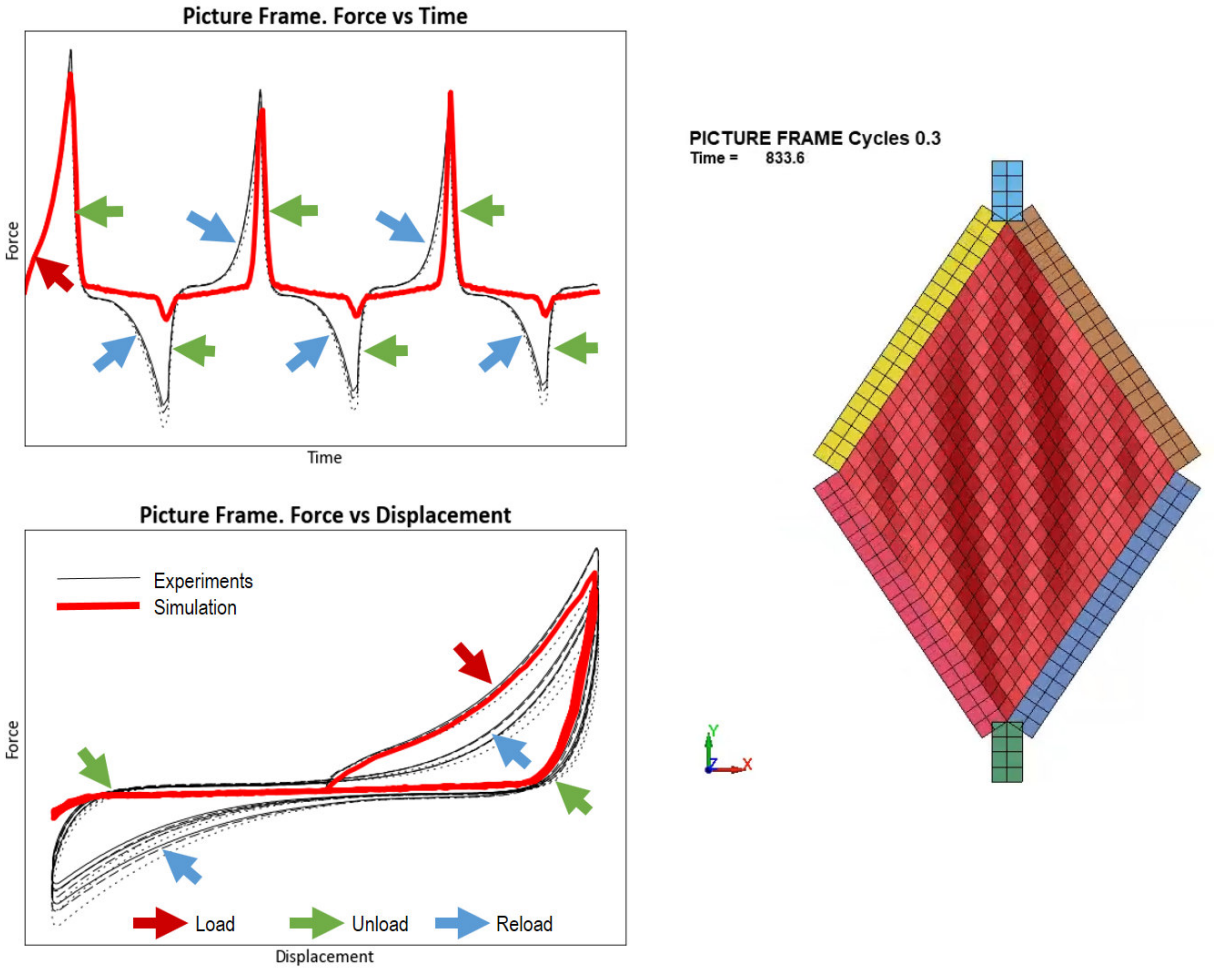

Fig.14: LS-DYNA models and typical validation results for picture frame tests.

Permeability Tests

Permeability tests are simulated in LS-DYNA using a numerical model of the complete experimental device. The setup is represented by two *AIRBAG_HYBRID cards, corresponding to the Pressure Vessel (Vol. 1) and the Test Chamber (Vol. 2), linked through an *AIRBAG_INTERACTION card that controls the gas exchange between both volumes. The model is initialized with the measured initial conditions of each chamber, without the use of an inflator. The same *MAT_FABRIC card previously calibrated against the mechanical tests of the material is applied, ensuring a realistic representation of the fabric deformation, while the pressure histories in both chambers (Vol. 1 and Vol. 2) are used for model validation (see Fig. 15).

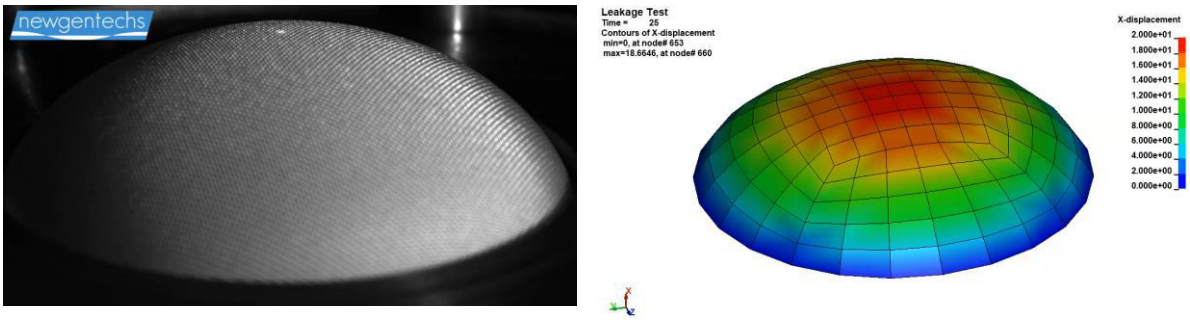

Fig.15: Physical shape of the bulge observed in a permeability tests and its numerical reproduction in the model.

To guarantee the reliability of the LS-DYNA models, a comprehensive calibration program was conducted using rigid specimens with predefined leakage areas, created by holes of known diameter, and tested under different pressure levels (see Fig. 16). This procedure enabled an accurate adjustment of valve parameters and discharge coefficients. The results confirmed that the adopted double-chamber configuration, together with the calibration method, reproduced the experimental system with high fidelity. Consequently, the use of a more complex airbag model was proven unnecessary.

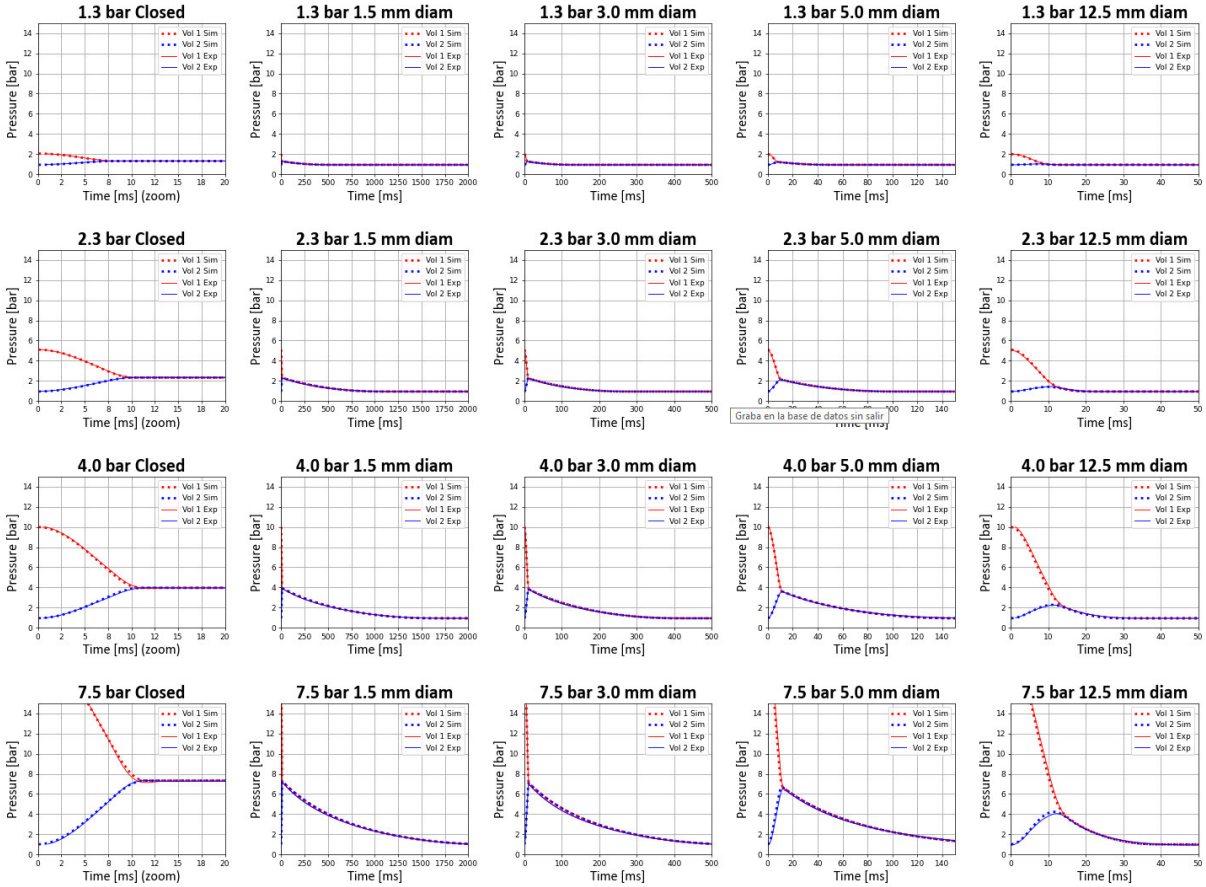

Fig.16: Results of the calibration program of the base Permeability models.

The direct implementation of the experimentally measured permeability curves into the FAC function of *MAT_FABRIC has been found to enable a proper reproduction of the experimental pressure decay in the permeability tests (see left graph in Fig. 17). However, the experiments also revealed the presence of permanent (plastic-like) strains in the fabric after high-pressure permeability tests. This is evidenced both by the comparison of experimental and numerical bulge height evolution (right graph in Fig. 17) and by the post-test observation of permanent deformation in the specimens (see Fig. 18). Such effects cannot be reproduced with the current *MAT_FABRIC formulation, since plastic strain is not implemented in the model. Although bulge height variations influence the calculation of the instantaneous test chamber volume and its exchange area with the atmosphere, this influence has consistently been found to be negligible for reproducing the pressure evolution. These results confirm that the proposed approach is suitable for incorporating permeability dependence into LS-DYNA material models, despite the absence of plastic strain representation.

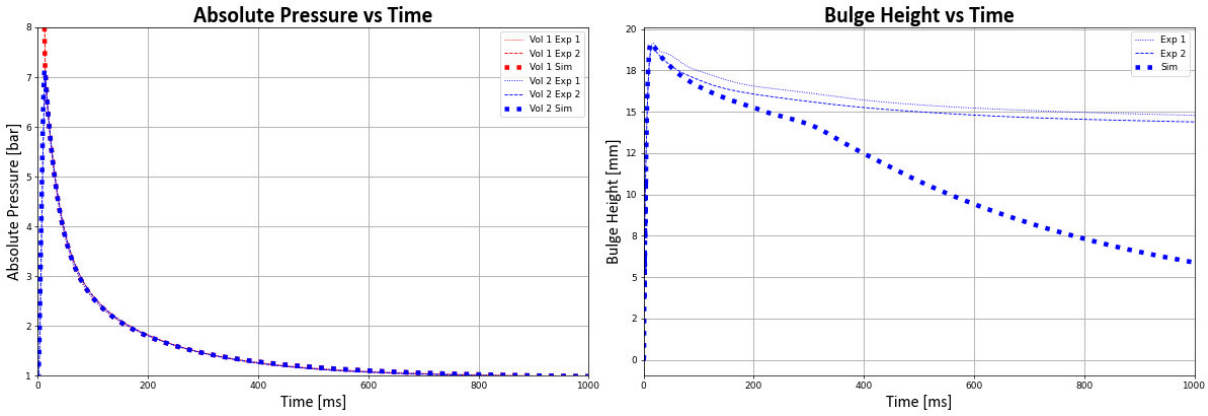

Fig.17: Validation of a permeability model (two repeated experiments displayed).

Fig.18: Permanent "plastic-like" strain after a permeability test.

8 Sensitivity analysis

In order to complete the presented information, a sensitivity analysis was carried out using the fictitious driver airbag model described before to illustrate the influence of different *MAT_FABRIC options on the simulation results. It is important to emphasize that this study must be regarded as an exploratory example. The use of different materials, geometries, or airbag types could lead to different numerical values or even conclusions.

Five alternative fabric material definitions were considered:

- **Base**: Standard complete definition including uniaxial and biaxial curves at different strain rates and permeability inputs.
- **Zero Porosity**: Uniaxial and biaxial inputs at different strain rates included, but no permeability.
- **Uniaxial Only**: Only uniaxial at different strain rates and permeability curves provided, without biaxial inputs.
- **Biaxial Only**: Only biaxial curves at different strain rates and permeability data included, without uniaxial inputs. In this case, the previous tables used for the biaxial values (LCAA and LCBB) have been directly introduced in the LCA and LCB positions.
- **No Strain Rate**: Strain rate independent models, substituting the tables LCA, LCB, LCAA and LCBB by the second curve of each table. This is aimed to reproduce a material with quasi-static information only.

These configurations are aimed to allow for the assessment of the relative importance of each modeling option and its contribution to the accuracy of the airbag simulation.

The sensitivity study was performed using the sample airbag models in four representative simulation scenarios: deployment with CPM, deployment with UP, restraint performance, and aggressiveness under out-of-position (OOP) conditions. The comparison of these configurations makes it possible to estimate how different definitions of fabric material models may influence the predictive accuracy of LS-DYNA simulations in other practical applications.

Deployment with CPM

The first case was conceived as a baseline, simulating the static deployment of an airbag initially placed in its housing and modeled with a detailed gas description using CPM. The objective was to assess how different fabric material definitions influence the early interaction with the cover as well as the final inflated shape of the airbag. Fig.19 shows the main results together with a sectional view of the deploying airbag.

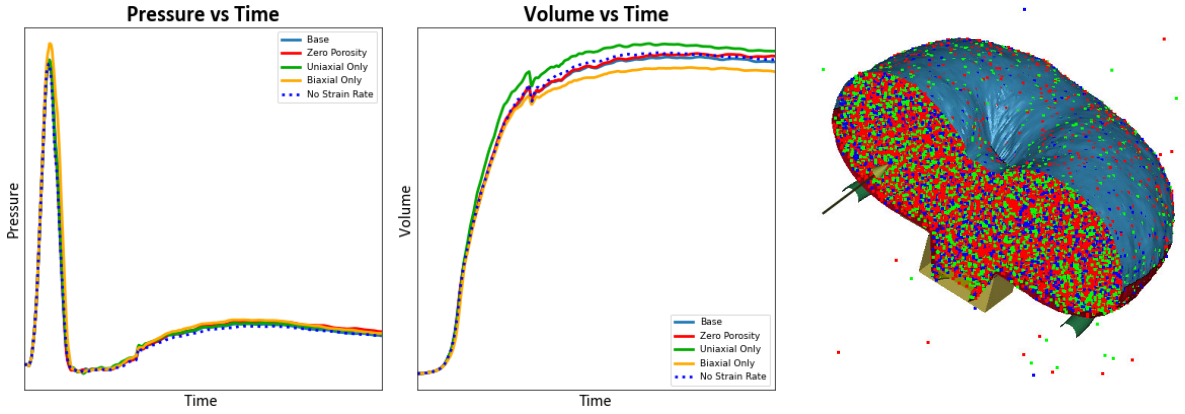

Fig.19: Main results and section view of the "Deployment with CPM" case.

In this configuration, porosity did not show a significant influence on global airbag behavior. However, the absence of either uniaxial or biaxial data in the fabric model led to differences of about ±4% in the final airbag volume. The "Biaxial Only" configuration showed slightly higher internal pressures during cover opening, with deviations of approximately +4% compared to the base case, and residual differences of about +2% after full inflation. These findings suggest that while deployment predictions of are not highly sensitive to porosity and strain rate (around 1% deviation in this example), the inclusion of both uniaxial and biaxial data is important to ensure accurate modeling of the bag volume evolution. These observations are in accordance with the higher stiffness of the biaxial curves with regards to the uniaxial curves, leading to slightly lower volumes both locally, just after the ignition, and once deployed.

Deployment with UP

The second case was also defined as a baseline, but using a simplified gas representation through the Uniform Pressure (UP) method. While the final deployment behavior and the homogenization of the internal pressure were expected to be comparable to CPM, the objective was to investigate potential differences during the initial phases of inflation. The main results are presented in Fig. 20.

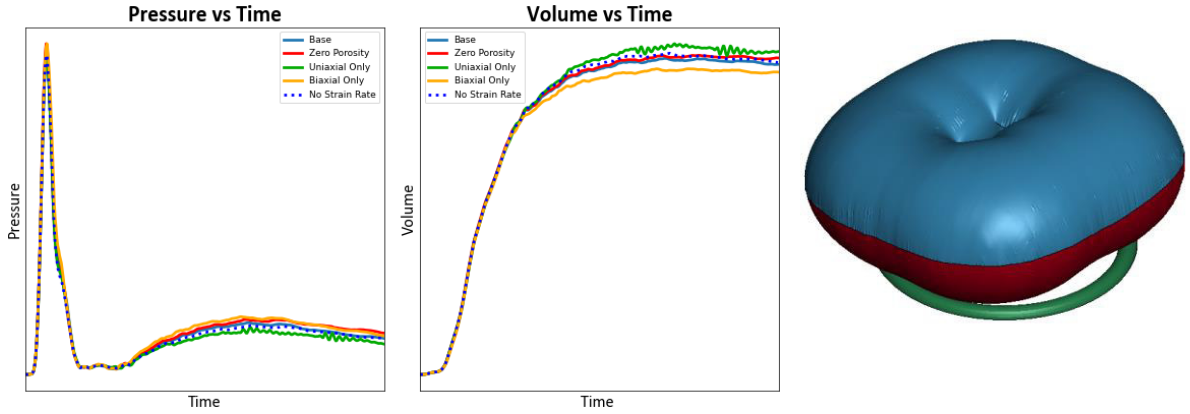

Fig.20: Main results and section view of the "Deployment with UP" case.

As expected, results after the airbag deployment were broadly consistent with those obtained with CPM. The "Biaxial Only" option again produced a slight increase in pressure during cover opening, though smaller than in CPM. On the other hand, permeability showed a higher influence, particularly on the pressure.

Restraint Performance

This case has been designed to represent the influence of the material model in a general case of occupant restraint during an impact situation. To this end, a 34 kg (~75 lb) guided mobile impactor with an initial velocity of 6.7 mm (~24 km/h or 15 mph), has been selected as representative. This situation reproduces an initial energy similar to those described by the ECE R12 [7], the FMVSS 203 [9] and the SAE J944 [9] standards. As the restraint function happens after de total deployment of the airbag, the Uniform Pressure gas definition was considered to be adequate. Fig. 21 shows the main results.

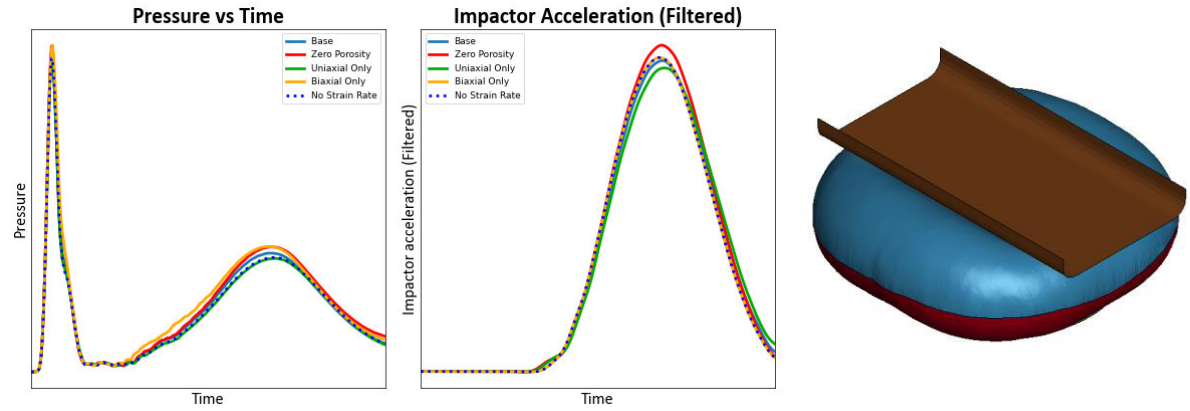

Fig.21: Main results and section view of the "Restraint Performance" case.

For this configuration, the acceleration of the impactor substituted the airbag volume as one of the main results to be considered. In this case, porosity emerged as the most influential parameter. Removing permeability increased the maximum impactor acceleration by up to 5%, highlighting its relevance for energy absorption and restraint efficiency. The lack of uniaxial, biaxial and strain rate data in the material definition produced variations of approximately 2% in pressure and acceleration. These effects, while modest, can still be relevant when fine-tuning restraint performance predictions. It is important to remind here that these findings can be different with other geometries, materials and load cases, so a personalized replication of this study is recommended for the particular application analyzed in each case.

Aggressiveness (Out-of-Position)

The aggressiveness analysis aims to simulate an Out-of-Position (OOP) condition, in which occupant interaction restricts the opening of the airbag cover. In this kind of situations the pressure in the airbag during the starting phases is expected to be much higher than in a common deployment. This case was targeted to analyse the influence of the material model under these over-presurized conditions. To represent the desired loads, a guided spherical impactor measuring Ø165 mm and weighting 6.8 kg (15 lb) was used and positioned next to the airbag cover with null initial speed. This impactor is representative of a free-motion head (FMH) used by several standards and testing procedures, including the ECE R21 [10], the FMVSS 201U [11] and the EURONCAP [12] among others. In this case, the detailed definition of the gas (CPM) was considered to be more adequate for the models. Main results are displayed in Fig. 22.

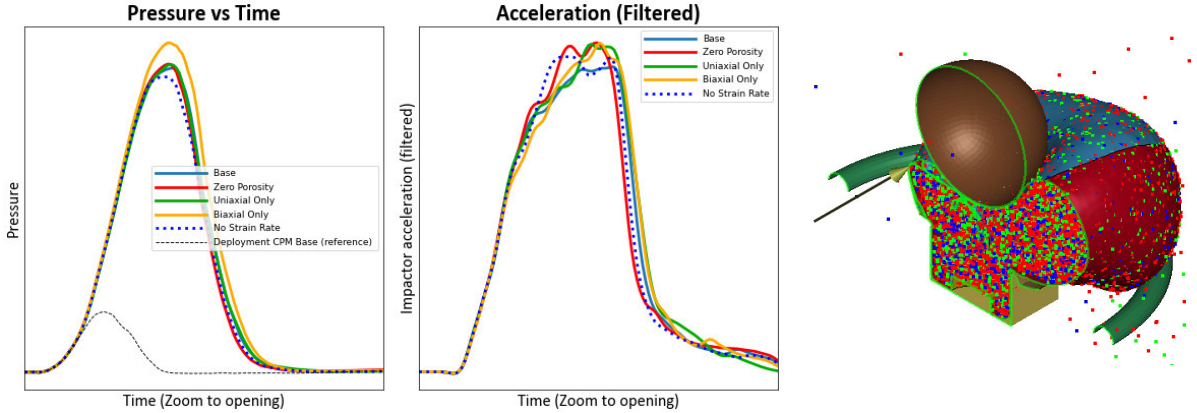

Fig.22: Main results and section view of the "Aggressiveness (Out-of-Position)" case. Pressure from the "Deployment with CPM" case is plotted also as a reference.

In this scenario, the acceleration curves are shown to be strongly affected by the different material definitions, with deviations of up to 6%. The largest deviations are associated with strain rate and porosity, being closely followed by the uniaxial and biaxial only definitions. Regarding average pressure, the "Biaxial Only" option exhibits the highest influence, with variations close to 8%.

Conclusion of Sensitivity Analysis

This sensitivity analysis demonstrates that the impact of fabric model definitions is not uniform, but depends strongly on the load case and the performance metrics considered. Porosity emerged as a relevant factor in restraint and OOP aggressiveness scenarios, where internal pressure governs occupant interaction and has a direct effect on impactor acceleration. Uniaxial and biaxial inputs primarily influenced the geometry of the deployed airbag, reflected in the predicted final volume, which in turn affected restraint performance. Strain-rate effects were most relevant under highly dynamic conditions, particularly during the opening and slash phases, but they also showed a measurable influence on restraint performance. This apparently small influence may become critical in high-accuracy applications, for example when results are close to regulatory assessment limits such as thorax intrusion.

It must be reminded here that the present sensitivity analysis is specific to the geometry and materials considered in this study. Different airbag types, materials, or loading conditions could lead to alternative results and conclusions. In general, for particular applications it is recommended to conduct a similar study using the specific models corresponding to the case under investigation.

Overall, the study confirms that each modeling option contributes in a distinct way to the predictive capability of LS-DYNA, highlighting the importance of a balanced, case-specific definition of material inputs. In practice, the conclusion is clear: achieving higher precision in airbag simulations requires providing a greater level of experimental detail in the material characterization.

9 Summary

In this work, some of the most advanced experimental techniques for the characterization of airbag fabrics have been reviewed, covering all the main dependencies implemented in *MAT_FABRIC and *MAT_FABRIC_MAP, namely uniaxial and biaxial loads, strain rate, temperature, and permeability at both low and high pressures.

The document highlights the main capabilities and limitations of *MAT_FABRIC, showing that while it can reproduce the essential mechanical response of fabrics, certain effects such as permanent strains or realistic histeresis in shear remain outside its scope.

It has also been presented an exploratory analysis of how different characterization options influence airbag simulations. The results show that each modeling approach contributes in a distinct way depending on the specific scenario considered, underlining that no single definition is universally optimal. It should also be noted that the conclusions may vary with different geometries, materials, or load cases; therefore, a tailored replication of this study is advisable for each particular application.

In general terms, the level of accuracy achieved in LS-DYNA predictions is directly linked to the level of detail included in the material definition, meaning that higher fidelity inevitably requires more comprehensive experimental input.

Finally, it can be helpful to remind that many of these methodologies, though focused here on airbags, are equally applicable to other fabrics used in restraint systems such as seat belts, offering a robust framework for reliable material modeling in LS-DYNA.

10 Literature

[1] “LS-DYNA Keyword User’s Manual, Volume II, Material Models.” LS-DYNA R16. 2015. Pages 312-355.

[2] Borrvall T., Ehle C., Stratton T.: “A Fabric Material Model with Stress Map Functionality in LS-DYNA”, 10th European LS-DYNA Conference, 2015.

[3] Muñoz D., Regidor A., Ferrer J. J. and Mansilla A.: “Use of 3D analytical surfaces (stress – strain – strain rate) in the materials characterization for crash simulation”, CARHS Automotive CAE Grand Challenge Conferences, 2014.

[4] Muñoz D., Regidor A., Ferrer J. J. and Mansilla A.: “Dynamic characterization of a plastic material by means of tensile tests and 3D analytical surfaces (stress - strain - strain rate)”, LS DYNA European Conference, 2013.

[5] Dörnhoff H., Regidor A., Muñoz D., Camarero A.: “Influence of the temperature on the dynamic mechanical properties and leakage properties of airbag fabrics” Airbag 2022 - 15th International Symposium and Exhibition on Sophisticated Car Safety Systems, 2022.

[6] “Standard Test Method for Determining Dynamic Air Permeability of Inflatable Restraint Fabrics”. ASTM International. Designation: D6476 − 12 (Reapproved 2017)

[7] United Nations Economic Commission for Europe. “Agreement concerning the Adoption of Uniform Provisions for Vehicle Approval with regard to the Protection of the Driver from the Steering Mechanism (ECE Regulation No. 12, Revision 4, Addendum 11)”, Ginebra: UNECE, 1995.

[8] National Highway Traffic Safety Administration (NHTSA). “49 CFR §571.203 - Standard No. 203; Impact protection for the driver from the steering control system”. Washington, DC: U.S. Department of Transportation. 2011.

[9] Society of Automotive Engineers (SAE). ”SAE J944: Steering Wheel Assembly Test Procedure”. Warrendale, PA: SAE International. 2018

[10] United Nations Economic Commission for Europe. “UN Regulation No. 21 – Uniform provisions concerning the approval of vehicles with regard to their interior fittings (E/ECE/324/Rev.1/Add.20/Rev.3). Ginebra: UNECE. 2019.

[11] National Highway Traffic Safety Administration. “49 CFR § 571.201 – Standard No. 201; Occupant Protection in Interior Impact (FMVSS 201U, Upper Interior Head Impact Protection)”. Washington, DC: U.S. Department of Transportation. 2018

[12] Euro NCAP. “Assessment Protocol – Vulnerable Road User Protection, Version 10.0.5 (Pedestrian Protection including Adult & Child Headform, Upper & Lower Legform Impact Devices)”. Bracknell, UK: Euro NCAP. 2021.